ASEAN Engineering Journal

Full Paper

DESIGN AND ANALYSIS OF LATERAL WALL DEFLECTION IN DEEP EXCAVATION ON SOFT CLAY: A CASE STUDY OF THE OPAL SKYVIEW BUILDING, HO CHI MINH CITY

ThiTuyetNga Phu[a], HongGiang Nguyen[b*]

[a]Institute of Architecture and Construction, ThuDauMot University, ThudauMot city 5500, Vietnam
[b]School of Engineering and Technology of Hue University, Hue City 49000, Vietnam

Article history
Received
09 January 2025
Received in revised form
23 May 2025
Accepted
28 May 2025
Published online
30 November 2025

*Corresponding author
giangnh@hueuni.edu.vn

Graphical abstract

Abstract

This study investigates the basement excavation of the Opal Skyview building in Thu Duc, Ho Chi Minh City, using 3D Plaxis numerical simulations for reverse analysis. The research aims to evaluate excavation behavior, particularly diaphragm wall displacement, by comparing numerical predictions with field monitoring data. The Hardening Soil (HS) and Mohr-Coulomb (MC) models were employed to simulate wall deflections at six monitoring locations (SID1–SID6) across various excavation stages. The results indicate that numerical simulations overestimated displacement at specific points, such as SID2 and SID6, by 1.3 and 1.1 times, respectively. The HS model demonstrated superior accuracy, closely aligning with observed data, whereas the MC model exhibited greater deviations. The findings highlight the critical role of accurate geotechnical investigations, appropriate design methodologies, and real-time monitoring in ensuring excavation safety and structural stability. Furthermore, the study underscores the necessity of integrating numerical simulations with field observations to enhance excavation efficiency and mitigate construction risks. By providing insights into excavation-induced deformations, this research contributes to more reliable and cost-effective deep excavation practices. The results serve as a valuable reference for engineers working on deep excavations in urban environments with complex geotechnical conditions.

Keywords: Excavation, Retaining wall, Hardening soil model, Mohr coulomb model, Soft clay soil.

1.0 INTRODUCTION

Deep excavation in soft clay soil conditions faces substantial challenges regarding safety, excavation stability, technical excavation processes, and high groundwater levels [1, 2]. Additionally, the capacity of deep excavation depends on several factors, including soil conditions, supporting systems, construction methods, the skill level of construction staff, and, notably, soil-structure interaction issues. These factors lead to many uncertainties in predicting the behavior of deep excavations. As a result, various techniques have been developed to assess the implementation of deep excavation in terms of horizontal wall movements, which will be described and discussed in this study.

However, deep excavation remains a necessary construction method for underground works, commonly used for basements of high-rise buildings, subway systems, and urban underground utilities. With the rapid development of the economy and urbanization, excavation projects are being carried out on a larger and deeper scale. In particular, some buildings are designed in challenging geological conditions, such as soft soils or hard-rock foundations. Ensuring the safety of the excavation and the surrounding structures presents a significant challenge for design and construction engineers. Therefore, new methods for designing and constructing deep excavations are crucial for ensuring safety and reducing construction costs.

Surface settlement and lateral wall displacement during the construction of a deep excavation are two crucial factors for

monitoring the excavation's behavior [3-5]. For example, Figure 1 shows wall deflection and ground movement induced by the excavation. Field monitoring aims to prevent large wall displacements and excessive ground-surface settlement, as these can negatively impact the safety of surrounding structures. The main factors influencing these issues include the geotechnical conditions of the construction site, the structural conditions of the excavation, and the technical aspects of the construction process [6, 7].

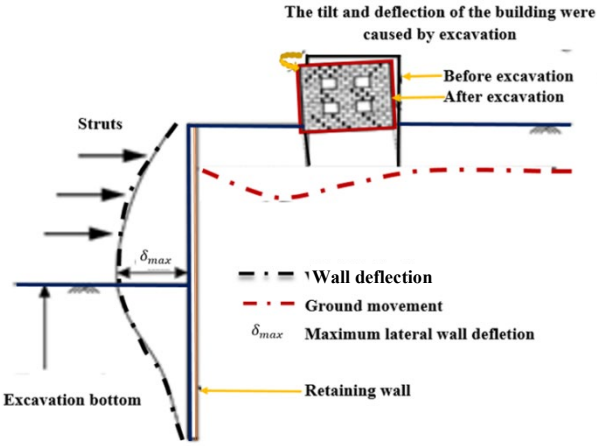

Figure 1 Wall deformation and ground displacement (Source: reference on [8])

Underground construction is a challenging problem that involves many complex issues related to engineering geology, hydrogeology, the foundation, and the basement. Therefore, an incorrect assessment of the relationship between these factors can lead to damage to the excavation. Common types of damage identified in studies include: failure of struts and walls, failure of ground anchors, wall leakage, failure of base soil, groundwater issues, uplifting, and settlement or sinkholes behind the wall [9-16]. As a result, extracting information to develop relationships between these factors requires advanced modeling techniques and expert knowledge.

In recent years, braced excavation has become common in construction. This method involves installing vertical members at regular intervals, and then placing a horizontal member between them to prevent wall deformation. Braced excavation can ensure safe excavation, stabilize narrow excavation sites, and reduce deformations in the surrounding ground caused by excessive wall deflections [17, 18].

Several technical methods for forecasting excavation wall deformation can be categorized into numerical simulation and empirical expressions [19-21]. Empirical expressions are based on historical sites and are relatively easy to model and implement [22-24]. In practice, numerical models are typically optimized for accuracy through reverse analysis of actual observations [25-27].

Regarding wall deflection, several studies have applied numerical methods using 2D and 3D Plaxis software to simulate inverse analysis and compare problems with design input data in order to optimize displacement analysis of diaphragm walls during excavation construction.

Hsiung et al. (2018) [27] deployed 3D simulations to model a large-scale deep excavation and its effect on wall deformation in Central Jakarta, Indonesia. This study simplified soil input parameters for the subsurface soil in Central Jakarta and evaluated deep excavation based on a 3D Plaxis model. The excavation method used was top-down, with a supporting system of concrete slabs, and the influence of the soil modulus was considered. The results indicated that the hardening soil model, with the soil modulus derived from in situ pressure meter tests, provided reasonable forecasts for excavation-induced wall deformation.

Hung et al. (2016) [28] reviewed 18 deep excavation projects in soft clay ranging from 4m to 16m thick in central Ho HCMC. Most projects used internally braced DWs, with maximum wall deflections ranging from 0.15% to 1.0%. A few projects applied sheet pile walls or micro-bored pile walls, with deflections between 1.0% and 2.4%. The study also found that the first excavation stage, using a cantilever mode, resulted in wall deflections of around 35% to 60% compared to the final stage. Furthermore, the study revealed that increasing the stiffness of the DW and bracing system was ineffective, while the DW was most effective in minimizing lateral wall displacement.

Duc et al. (2022) [29] used the FEM with the MC and HS models to certify parameter meters and the correlation coefficient (E_{oed}/E_{50}) for soft soil in HCMC, based on Oedometer tests for deep excavation calculations. The results showed that the HS model, relying on the hyperbolic model, performed better than the MC model. The HS model also described the dependence of the modulus on stress, with the degree of stress dependence given by the exponent m, and the parameter was verified based on the HS model.

Nguyen et al. (2022) [30] presented a case study of ground surface and DW deformation during the construction of the first metro line in HCMC. The deformation behavior of the deep excavation retained by the DW was analyzed using finite element analysis in Plaxis. The numerical results showed that the lateral displacement of the DW significantly declined when the water table was drawn down during the dry season. The study also recommended that changes in the water table level throughout the seasons should be considered during the deep excavation phase in HCMC.

Lai et al. (2020) [31] studied the combination of DWs and SP-walls to deepen the basement of a high-rise building project in HCMC. Plaxis 2D model was used to evaluate the behavior of this combination using FEM analysis. The lateral wall deflection from the analysis was compared to field observations, and the results showed good agreement between the forecasting simulations and the monitoring values.

HCMC is a pillar of and a driving force behind the current economic development of Vietnam. In recent years, the demand for high-rise apartments with basements has continuously increased in the city. When designing and constructing high-rise buildings with basements, retaining walls, and deep excavations, it is essential to assess wall displacement. Incorrect calculations can lead to damage to neighboring structures and ongoing works, negatively impacting the structural functions and durability of the building itself [32-34].

The Opal Skyview building is a modern apartment complex located in Thu Duc, HCMC. The construction of its basement is particularly complex. As part of this project, numerical simulation using 3D Plaxis was applied to reverse analysis problems, with input data for the simulation evaluating diaphragm wall displacement during excavation. The actual horizontal wall displacements at the monitoring points were compared with the simulation results to help optimize the analysis of excavation behavior during construction. The findings

from this analysis may provide optimal architectural solutions to ensure bearing capacity and reduce construction costs. To ensure safe construction, the contractor used six key locations on the foundation to monitor horizontal displacement, using the collected data for numerical simulation through reverse analysis.

This study proposes a dynamic estimation algorithm for determining maximum wall deflections in braced excavations in soft clay. Initially, wall deflection conditions were monitored to collect a reliable dataset. Next, the monitored data were compared with simulation results from the HS and MC models. Finally, the study suggests that the optimal performance model could serve as a practical method for calculating maximum wall deflections and their positions.

2.0 METHODOLOGY

2.1. The Project Site's Description

The project site is located in Quarter 9, Hiep Binh Chanh Ward, Thu Duc Town, HCMC (as shown in Figure 2). The total project area is approximately 3,326 m², with an estimated construction area of around 18,002 m², including twenty-one floors and two basements. The site is situated in an unfavorable geological area, with a 26-meter thick silt clay layer. Figure 3 displays the geological layers based on engineering geological cross-sections from three drill holes: HK1, HK2, and HK3.

Figure 2 Project location and Opal Skyview building

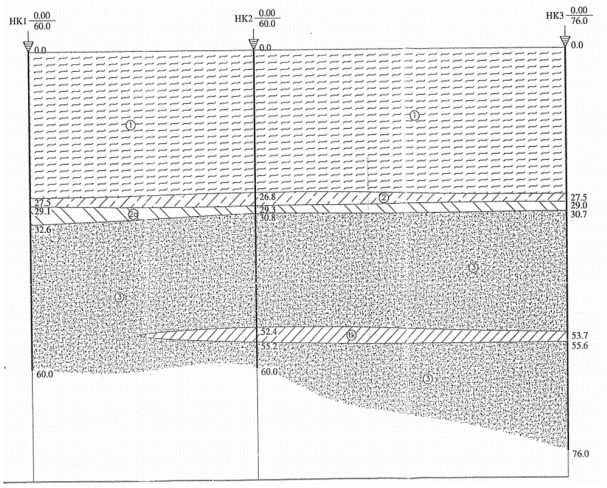

Figure 3 Engineering geological cross-section

Layer 1: Blue-gray, dark-gray organic composition of silt clay, fluid-plastic state;
Layer 2: Gray-brown, gray-white sand clay, soft-plastic state;
Layer 2a: Dark gray-green, hard plastic state;
Layer 3 : White gray, light yellow brown, light pink medium dense sand; medium-plastic state;
Layer TK: Reddish brown, yellow brown clay, quasi-plastic state.

The lateral displacements of the deep excavations were monitored by the 6 inclinometers which were installed in the retaining wall as shown in Figure 4 These monitoring data are used as the basis for the reverse analysis problem in the study process.

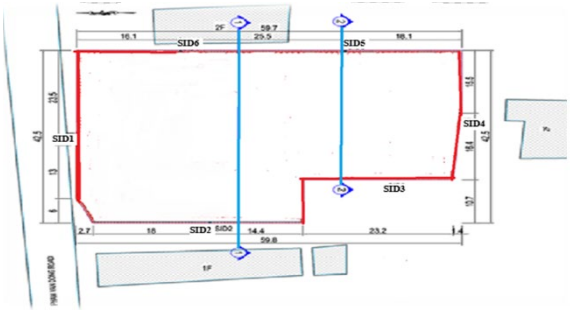

Figure 4 Plan view of the construction

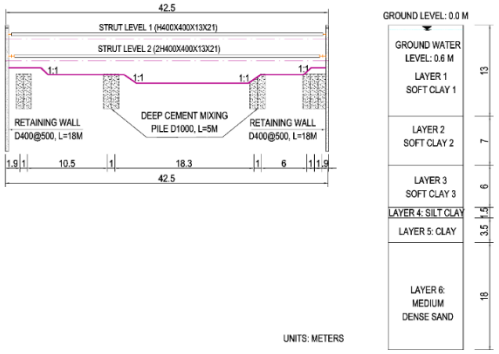

Figure 5 Cross-section of deep excavation: section 1-1.
Source: reference on [35]

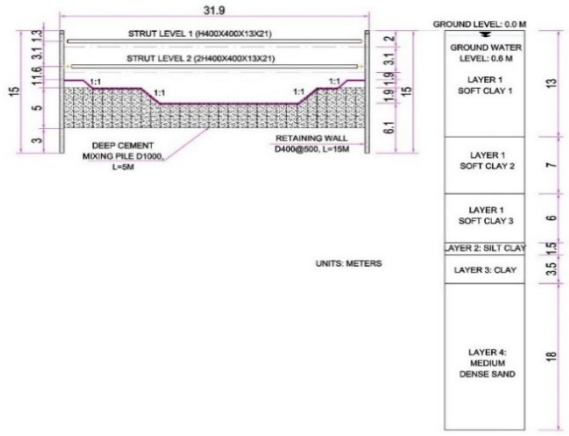

Figure 6. Cross-section of deep excavation: section 2-2

Figures 5-6 show two main sections (1-1 and 2-2) used to evaluate the behavior of the excavation pit during construction using the bottom-up method. Section 1-1 passes through the position of the elevator pit. The excavation depth from the ground surface to the bottom of the edge foundation is 6 meters, with the bottom of the elevator pit at 8.2 meters. The existing diaphragm pile wall is D400@500, with a pile length of 18 meters. Section 2-2 passes through the location of the underground water tank, where the excavation depth from the ground surface to the bottom of the edge foundation is 6 meters, and the bottom of the underground water tank is at 8.8 meters. The existing diaphragm pile wall in this section is D400@500, with a pile length of 15 meters. Both sections are reinforced with soil CDM piles, which extend to a depth of 7 meters from the ground surface, with CDM piles having a length of 5 meters. These piles help prevent damage to the foundation pile system by using a combination of struts to stabilize the excavation hole. The main steps in the excavation process are as follows: *Stage 1:* Load assignment and CDM pile construction. *Stage 2:* Excavating soil for the first time to the level of the 1st basement. *Stage 3:* Installing Strut brace 1 (H400). *Stage 4:* Excavating the soil layers for the second time to the level of the 2nd basement. *Stage 5:* Installing Strut brace 2 (2H400). *Stage 6:* Excavating the soil layers for the third time to reach the bottom of the foundation, including the elevator pit and water tank.

2.2 The Mohr-Coulomb Model

The plasticity model of Mohr-Coulomb is usually used in sand behavior simulation to resolve geotechnical engineering problems [36-38]. The model is incorporated linear isotropic elasticity Hooke's law and Coulomb's failure criterion [39-41], and the formula of the criterion may be described as below:

$$\tau_f = \sigma'_{nf} tan\emptyset' + c' \qquad (1)$$

where, τ_f, σ'_{nf}, $\emptyset'$, c'*are* shear stress at failure plane, normal effective stress at failure plane, effective friction angle, and cohesion, respectively.

In addition, the model is applied to Plaxis software which has at least six parameters see Table 1.

Table 1 Input parameters for MC model

Parameter	Description
$\emptyset'$	Internal friction angle
c'	Cohesion
ψ	Dilatancy angle
E_{50}	Secant stiffness from drained triaxial test
v	Poisson's ratio
K_o^{nc}	Coefficient of at rest earth pressure (NC state default setting, 1-sin ϕ')

2.3 The Hardening Soil Model

The hardening soil model consists of shear hardening to model the irreversible plastic deformation in deviatoric loading and compressive hardening to model the irreversible volumetric strain in primary compression in loading of oedometer and isotropic [42-44]. The failure criteria are verified utilizing the MC failure criteria. Hardening is presumed to be isotropic, relying on the plastic shear and volumetric deformation [45, 46]. A non-associated flowing formula is deployed when associated frictional hardening; at the same time the related flow rule is supposed for the cap hardening [47, 48]. The HS model replaces the hyperbolic model by using the plasticity theory instead of the elasticity theory by using soil dilatancy and describing a yield cap to compress hardening [43, 46, 49, 50]. In the HS model, there are ten input parameters as detail in Table 2.

Table 2 Input parameters for HS model

Parameter	**Description**
$\emptyset'$	Internal friction angle
c'	Cohesion
ψ	Dilatancy angle
K_o^{nc}	Coefficient of at rest earth pressure (NC state default setting, 1-sin ϕ')
R_f	Failure ratio, $(\sigma_1-\sigma_3)f/(\sigma_1-\sigma_3)ult$
E_{50}^{ref}	Reference secant stiffness from drained triaxial test
E_{oed}^{ref}	Reference tangent stiffness for oedometer primary loading
E_{ur}^{ref}	Reference unloading/reloading stiffness
m	Exponential power
v_{ur}	Unloading/reloading Poisson's ratio, 0.2 (default setting)

The confining stress of E_{50} and E_{ur} are dependent on stiffness module for initial loading and unloading/reloading to derive from drained triaxial test; the parameters of reference oedometer moduli E_{ur}^{ref}, and E_{oed}^{ref} deployed to supervise the magnitude of the plastic deformation volumetric hardening. They get the formula below:

$$E_{50} = E_{50}^{ref}\left(\frac{c'cos\emptyset' - \sigma_3' sin\emptyset'}{c'cos\emptyset' + p^{ref} sin\emptyset'}\right) \qquad (2)$$

$$E_{ur} = E_{ur}^{ref}\left(\frac{c'cos\emptyset' - \sigma_3' sin\emptyset'}{c'cos\emptyset' + p^{ref} sin\emptyset'}\right) \qquad (3)$$

$$E_{oed} = E_{oed}^{ref}\left(\frac{c'cos\emptyset' - \sigma_1' sin\emptyset'}{c'cos\emptyset' + p^{ref} sin\emptyset'}\right) \qquad (4)$$

$$E_{ur,oed} = E_{ur}^{ref}\left(\frac{c'cos\emptyset' - \sigma_1' sin\emptyset'}{c'cos\emptyset' + p^{ref} sin\emptyset'}\right) \quad (5)$$

where, E_{oed} and σ_1' are tangent stiffness modulus, and the effective consolidation stress in oedometer test, respectively, in addition, σ_1' value is negative in compression.

In Plaxis simulation software, several indicators are default settings such as p^{ref} = 100 kN/m², σ'_3 is negative in compression, m ranges from 0.5 (for sand) to 1 (for soft soil) in different soil types, and E_{ur}^{ref} = $3E_{50}^{ref}$ (average value for kind of soil types) [17].

2.4 Creating Simulation

The 3D Plaxis software is carried out in the sequence of steps with the groundwater level 0.6m below ground level, such as (i) creating a ground model, (ii) creating a structural model for the excavation, (iii) analyzing the mesh model, (iv) simulation of hydrological conditions, and (v) simulation of excavation construction steps. The boundary dimensions should include X, Y and Z were 220m, 51.5m, and 50m, respectively. In addition, the simulation method is bottom-up. The simulation steps are shown in the Figure A1 – A7.

2.5 Experiment

The parameters of ground soil, CDM, diaphragm wall structure, and strut system are shown in Tables 3–6 and Figure 7, specifically as follows:

Table 3 Synthesize soil parameters

Soil Layer	Soft Clay 1	Soft Clay 2	Soft Clay 3	Silty Clay	Clay	M.D.S
Thickness (m)	13	7	7	1.5	3.5	18
γ_unsat (kN/m³)	14.2	14.2	14.2	19	19.15	19.1
γ_sat (kN/m³)	16.2	16.2	16.2	19.5	19.45	20.34
C (kN/m²)	9	11	15	9.1	26.4	3.2
$\varphi^{(0)}$	25.6	25.2	25	18	13.8	26
E^{ref}_{50} (kN/m²)	4430	5681	7232	28348	34095	31500
E^{ref}_{oed} (kN/m²)	2215	2990	3806	16675	20056	21000
E^{ref}_{ur} (kN/m²)	13069	16147	20554	83375	100280	63000
Liquid Limit (%)	65	51	82	-	-	-
Plastic Limit(%)	41	35	45	-	-	-
Drained Type	U(A)	U(A)	U(A)	U(A)	U(A)	D

Table 4 Synthesize CDM parameters

Soil	γ(kN/m³)	c(kN/m²)	$\varphi^{(0)}$	E (kN/m²)
CDM	16.1	43.9	2.7	34,725

Table 5 Synthesize strut parameters

Level	Strut size	EA (kN/m)	L spacing (m)
1	400x400x13x21	4.15 x 10⁶	7
2	2400x400x13x21	8.3 x 10⁶	7

Table 6 Diaphragm wall type

No.	Parameter	Value	
		D400@500	D500@600
1	Diameter (m)	0.4	0.5
3	Shear strength (Mpa)	28	28
4	Young's Module (kN/m²)	2.850E+07	3.00E+07
5	Cross-section (m²)	0.126	0.196
6	Moment of inertia (m⁴)	1.257E-03	3.068E-03
7	Axial stiffness (kN/m)	7.29E+06	1.00E+07
8	Bending stiffness (kNm²/m)	7.29E+04	1.56E+05

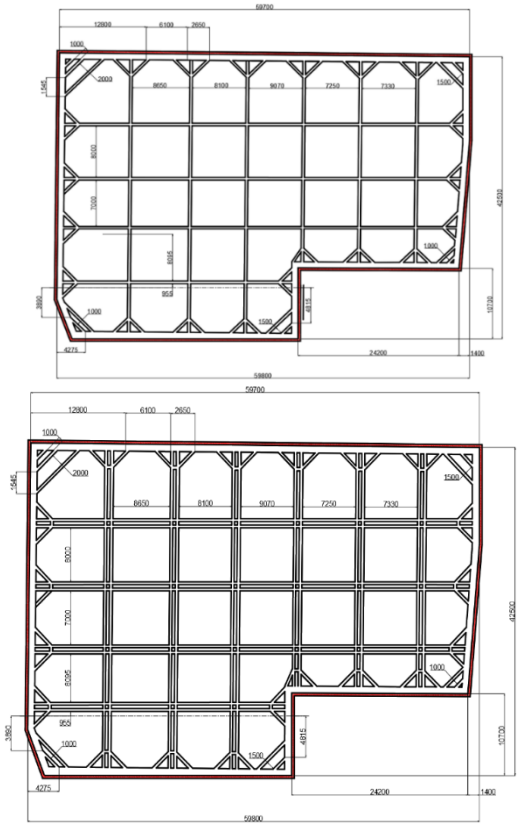

Figure 7 The structure of struts of level 1 and level 2

3.0 RESULTS AND DISCUSSION

The six-line charts in Figure 8 indicate the results of wall deflection from HS, MC models, and observation. The horizontal displacement of the wall through the 6 measuring points of the simulation value range of both models to compare with the monitor values. The detail at six monitoring locations from SID1 to SID6, the numerical simulation results in excavation phase 1, excavation phase 2, and excavation phase 3 are quite similar to the monitoring results. However, at monitoring location SID2, the numerical simulation results in the excavation of stage 2 simulation of both of models are higher than that of observation about 1.3 times; at the same time, at monitoring location SID6, excavation of stage 3 gives a value about more 1.1 times larger than the observed value (overestimated). In addition, the simulation value ranges of the HS model are more accurate than the MC models

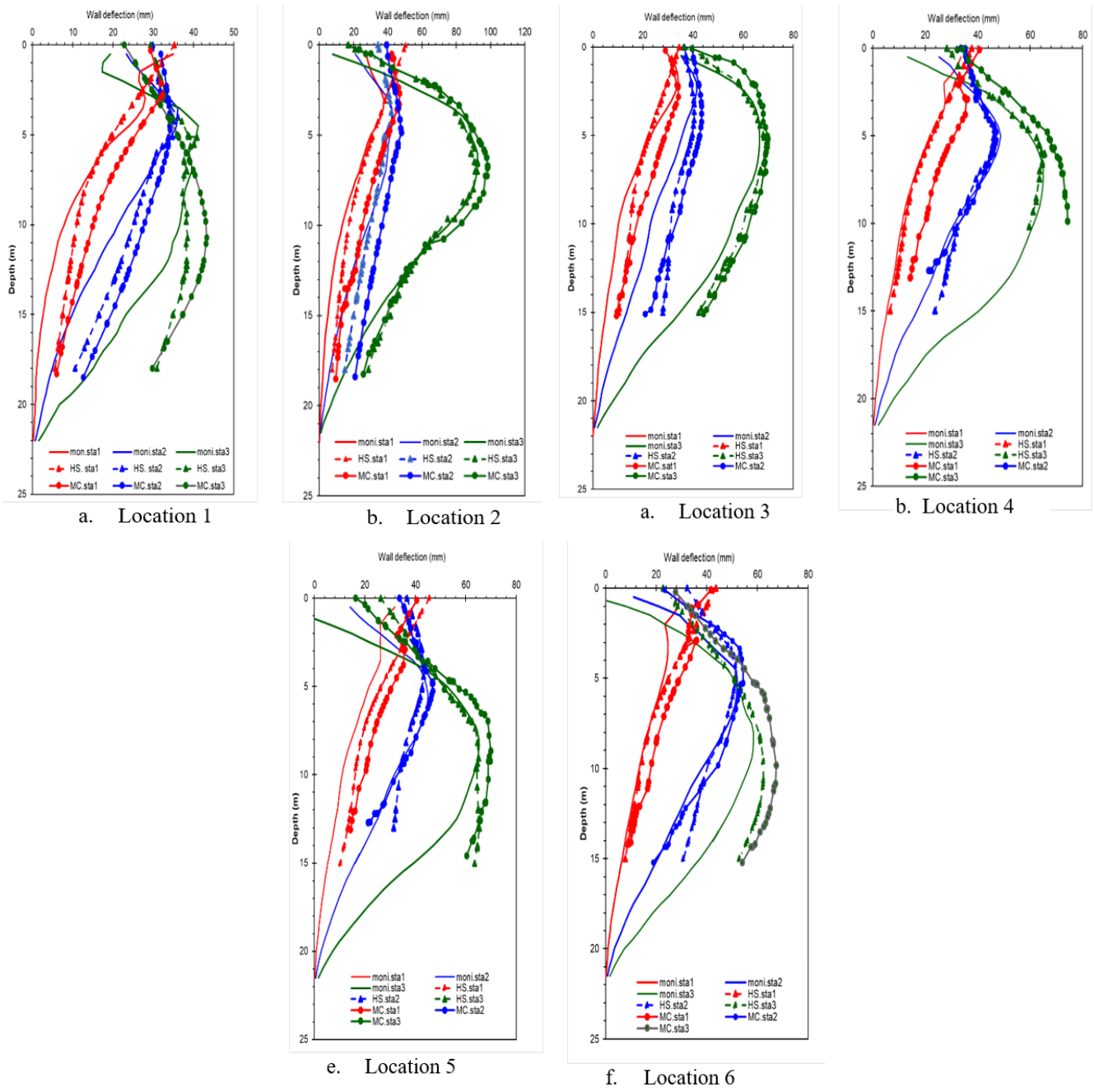

Figure 8 Wall deflection from HS, MC models, and observation

Excavation incidents in several high-rise construction projects in HCMC are attributed to various factors, primarily inaccurate ground surveys, faulty designs, deviations from approved construction plans, inadequate quality assurance, insufficient monitoring, and poor management. Given these risks, careful consideration in the design and construction of excavation pits is essential to prevent structural failures and associated hazards.

During the design phase, engineers must collect comprehensive and accurate geotechnical data, hydrological information, and details on adjacent structures. Simulating excavation behavior through experimental or numerical methods ensures structural safety, optimizes design efficiency, and helps reduce construction costs. Additionally, numerical simulation is applied in backward analysis comparison problems, with design input data optimized by analyzing excavation behavior during construction. For this study, the HS model and bottom-up excavation methods were used to analyze excavation behavior. The soft clay layer in the project was divided into three layers in the numerical simulation to reflect the increasing ground stiffness with depth, based on previous research results for the geology of HCMC. For the CDM system, the pile values were used to accurately assess the influence of the pile on wall displacement.

Field measurements and numerical simulations using 3D Plaxis indicate that the displacement error is within an acceptable range. However, to provide a more objective evaluation of numerical simulations and assess their applicability to real-world projects, this study collected displacement data from seven high-rise buildings in HCMC with basement depths comparable to the test project. This comparison helps evaluate the reliability of the simulation methods and their practical implementation in construction projects. Hence, the data presented in Table 7 show that the δH/He ratio for maximum wall deflection, based on monitoring and simulation data at an excavation depth of less than 7m, is 1.04 and 1.02, respectively. These values fall within the 0.3%–2.4% range for maximum lateral deflection in deep excavations in central HCMC, as observed in cases involving internally braced diaphragm walls, sheet pile walls, or micro-bored pile walls. Therefore, this study employs inverse analysis using 3D Plaxis simulations to achieve an acceptable level of accuracy.

Table 7 Fundamental dataset of deep excavations and HS model of the research in HCMC center of soft clay

Name	Method	Type	Hw (m)	He (m)	t (m)	B x L (mxm)	Number of bracings	δH (mm)	δH/He (%)
1. Sunrise City-Plot V-D7	TD	DW	54	13.5	0.8	80 x160	2	78	0.5
2. Cantavil Complex-D2	TD	DW	21	14.5	0.8	68x165	2	50	0.3
3. Blooming Park Towers-D2	BU	SPW	18	7	0.4	120x170	2	172	2.4
4. Thanh Da view-BT	BU	DW	22	11	0.6	47x56	2	33	0.3
5. Saigon Pearl-BT	BU	BPW	18	11	0.4	35x96	2	120	1
5. Phu My Thuan-NB	BU	BPW	12	8	0.3	60x150	2	158	1.9
6. Deawon-Hoancau Building-BT	BU	SPW	24	12	0.4	56x65	2	118	1
7. Opal Skyview Building	BU	BPW	18	8.9	0.4	42.5x60	2	92.39	1.04
8. Opal Skyview Building (Hs model)	BU	BPW	18	8.9	0.4	42.5x60	2	90.35	1.02

Source: reference on [28]

In excavation constructions, observational methods were related to assuring safe construction, as well as deployed a finite element to predict wall deflections in excavations. Hence, the set of tools that have been built for this project, it will help the construction contractors that basing on the study results to come up with many construction methods for the constructions of high-rise building in the next time in the project planning without having to spend a lot of money and time on field experiments in particular, and this is a useful reference channel for engineers when designing similar deep excavations to evaluate input parameters of stiffness modulus for the ground as well as the behaviour of the deep excavation such as wall displacement and surrounding ground settlement by general simulation. In addition, the HS model was used to calculate the inverse model for this deep excavation work. In terms of computational methods, these machine learning and deep learning models was deployed to train the relationship between the soil stiffness modulus and wall of maximum displacement and its position to minimize reduction with the difference between the machine learning model and the field observations caused by the excavation process. Since geotechnical engineers are faced with complex multivariate problems during the design and implementation of excavation, involving several interacting factors, in general, the relationship between these factors is not precisely known, in particular. Therefore, this study has shown the relationship between the main factors that will make it easier for them to set up a model of excavations with equivalent construction techniques and properties of soil layers. Moreover, this construction method has helped the building implementation to be safe and minimize the negative impact on neighbors' buildings. In addition, the city government needs to develop a geological guidebook to serve the infrastructural construction.

4.0 CONCLUSION

In the numerical simulation, the soft soil layer in this research project is divided into three sublayers to account for the increasing soil stiffness with depth, based on previous geological studies of HCMC. The detail of the CDM system indicates that CDM distribution covers approximately 50% of the foundation ground, resulting in negligible error in predicting the displacement of the fin pile compared to actual construction data.

The HS model is utilized for 3D simulations at six monitoring points (SID1 to SID6). The simulation results demonstrate that the predicted values at monitoring locations SID1 to SID6, at excavation depths of 2.1m, 5.1m, 7m, 8.2m, and 8.9m, closely match the observed values. For high-rise buildings, construction contractors must monitor the vertical displacement of the ground behind the diaphragm wall to assess and estimate the extent of deformation affecting adjacent structures. Therefore, computer-based simulations are essential for analyzing, evaluating, and estimating the influence radius and vertical displacement behind the diaphragm wall before construction begins. However, throughout the construction process, field measurements and observations remain necessary to obtain accurate and complete data for comparison with simulation results, ensuring potential technical issues are addressed effectively.

This study primarily focuses on variations in the physical and

mechanical properties of the soil and the strut system under the bottom-up excavation method. To enhance predictive accuracy, alternative machine learning models could be applied to estimate additional ground forces and refine input parameters for displacement calculations.

3D Plaxis software has been extensively studied and successfully applied to geotechnical design and construction. However, its accuracy is highly dependent on the precision of input data, particularly in soil sampling and laboratory testing, which must meet the software's technical requirements.

Abbreviation

3D	Three-dimensional
ε	Epsilon
γ	Total unit weight of soil (kN/m^3)
γ_unsat	Soil unsaturated unit weight (kN/m^3)
γ_sat	Soil saturated unit weight (kN/m^3)
ν	Poisson's ratio of soil
$\varphi^{(0)}$	Friction angle of soil
δH	Maximum lateral wall movement (mm)
$_{\beta}$H	Lateral wall deflection/Wall deflection (mm)
A	Cross-section (m^2)
B	Excavation width (m)
BU	Bottom-up
C	Cohesion (kN/m^2)
CDM	Cement Deep Mixing
DW	Diaphragm wall
E	Young's modulus of soil (kN/m^2)
EA	The axial stiffness (kN/m)
EI	Bending stiffness (kN/m)
E^{ref}_{50}	Reference secant stiffness from drained triaxial test (kN/m^2)
E^{ref}_{oed}	Reference tangent stiffness for oedometer primary loading (kN/m^2)
E^{ref}_{ur}	Reference unloading/reloading stiffness (kN/m^2)
FE	Finite element
FEM	Finite Element Method
HCMC	Ho Chi Minh City
H	Excavation depth (m)
He	Final excavation depth (m)
Hi	Depth of measuring points (m)
HK	Drill hole
HS	Hardening Soil model
HS.sta 1	Hardening soil model data at 2m excavated stage
HS.sta 2	Hardening soil model data at 5.1m excavated stage
HS.sta 3	Hardening soil model data at under 7m excavated stage
I	Moment of inertia (m^4)
IF	Instance Frequency
K_0	Coefficient of lateral earth pressure of soil
L	Excavation length (m)
LL	Liquid Limit (%)
MC	Mohr-Coulomb
MC.sta 1	Mohr-Coulomb model data at 2m excavated stage
MC.sta 2	Mohr-Coulomb model data at 5.1m excavated stage
MC.sta 3	Mohr-Coulomb model data at under 7m excavated stage
moni.sta 1	On site monitor data at 2m excavated stage
moni.sta 2	On site monitor data at 5.1m excavated stage
moni.sta 3	On site monitor data at under 7m excavated stage
PL	Plastic Limit (%)
S	The vertical distance of two strut frames (m)
SID	Inclinometer in pile retaining wall
SPT	Standard Penetration Test
Su	Undrained shear strength of clay (kN/m^2)
SP-wall	Secant piles wall
t	Wall thickness (m)
TD	Top-down

Acknowledgement

Thanks for group research number of NCTB.DHH.2024.05 of Hue University.

Conflicts of Interest

The author(s) declare(s) that there is no conflict of interest regarding the publication of this paper.

References

[1] Hou, Y., Fang, Q., Zhang, D., & Wong, L. N. Y. 2015. Excavation failure due to pipeline damage during shallow tunnelling in soft ground. *Tunnelling and Underground Space Technology,* 46: 76-84. DOI: https://doi.org/10.1016/j.tust.2014.11.004.

[2] Shreyas, S. K., & Dey, A. 2019. Application of soft computing techniques in tunnelling and underground excavations: state of the art and future prospects. *Innovative Infrastructure Solutions*, 4(1): 46. DOI: https://doi.org/10.1007/s41062-019-0234-z

[3] Bhatkar, T., Barman, D., Mandal, A., & Usmani, A. 2017. Prediction of behaviour of a deep excavation in soft soil: a case study. *International Journal of Geotechnical Engineering,* 11(1): 10-19. DOI: https://doi.org/10.1080/19386362.2016.1177309

[4] Ou, X., Zhang, X., Fu, J., Zhang, C., Zhou, X., & Feng, H. 2020. Cause investigation of large deformation of a deep excavation support system subjected to unsymmetrical surface loading. *Engineering Failure Analysis,* 107: 104202. DOI : https://doi.org/10.1016/j.engfailanal.2019.104202.

[5] Xu, Q., Xie, J., Zhu, H., & Lu, L. 2024. Supporting behavior evolution of ultra-deep circular diaphragm walls during excavation: Monitoring and assessment methods comparison. *Tunnelling and Underground Space Technology*, 143: 105495. DOI: https://doi.org/10.1016/j.tust.2023.105495.

[6] Ou, C. Y. 2014. *Deep excavation: Theory and practice*. Crc Press. DOI: https://doi.org/10.1201/9781482288469.

[7] Paraskevopoulou, C., & Boutsis, G. 2020. Cost overruns in tunnelling projects: Investigating the impact of geological and geotechnical uncertainty using case studies. *Infrastructures,* 5(9): 73. DOI: https://doi.org/10.3390/infrastructures5090073.

[8] Kung, G. T., Hsiao, E. C., Schuster, M., & Juang, C. H. 2007. A neural network approach to estimating deflection of diaphragm walls caused by excavation in clays. Computers and Geotechnics, 34(5): 385-396. DOI: https://doi.org/10.1016/j.compgeo.2007.05.007.

[9] Moh, Z. C., & Hwang, R. N. 2005. Geotechnical considerations in the design and construction of subways in urban areas. In *Seminar on Recent Developments on Mitigation of Natural Disasters, Urban Transportation and Construction Industry,* 30.

[10] Anggraini, R., Tavio, T., Raka, G. P., & Agustiar, A. 2021. Experimental load-drift relations of concrete beam reinforced and confined with high-strength steel bars under reversed cyclic loading. *ASEAN Engineering Journal,* 11(4): 56-69. DOI: https://doi.org/10.11113/aej.v11.17864

[11] Fajri, A., Suryanto, S., Adiputra, R., Prabowo, A. R., Tjahjana, D. D. D. P., Yaningsih, I., ... & Soedjarwo, M. 2024. Tensile assessment of woven CFRP using finite element method: A benchmarking and preliminary study for thin-walled structure application. *Curved and Layered Structures*, 11(1): 20240002. DOI: https://doi.org/10.1515/cls-2024-0002.

[12] Tran-Nguyen, H. H. (2014). Remedial structures to stabilize Long Xuyen riverbank to prevent sliding in An Giang province, Vietnam. *ASEAN Engineering Journal,* 3(2): 42-54. DOI: https://doi.org/10.11113/aej.v3.15524.

[13] Teparaksa, W. 2011. Performance of contiguous pile wall for deep excavation on chao phraya river bank. ASEAN Engineering Journal, 1(3): 6-31. DOI: https://doi.org/10.11113/aej.v1.15297.

[14] Sagitaningrum, F. H., Kamaruddin, S. A., Nazir, R., Soepandji, B. S., & Alatas, I. M. 2024. Interface Shear Strength Degradation In Progressive Landslide Of Weathered Clay Shale Overburden On Undisturbed Clay Shale. ASEAN Engineering Journal, 14(1): 11-17. DOI: https://doi.org/10.11113/aej.v14.18154.

[15] Coda, S., Tessitore, S., Di Martire, D., Calcaterra, D., De Vita, P., & Allocca, V. 2019. Coupled ground uplift and groundwater rebound in the

metropolitan city of Naples (southern Italy). *Journal of Hydrology*, 569: 470-482. DOI: https://doi.org/10.1016/j.jhydrol.2018.11.074.

[16] Mair, R. J. 2013. Tunnelling and deep excavations: Ground movements and their effects. In Proceedings of the *15th European Conference on Soil Mechanics and Geotechnical Engineering*. 39-70. IOS Press. DOI: 10.3233/978-1-61499-199-1-39.

[17] Yong, C. C., & Oh, E. 2016. Modelling ground response for deep excavation in soft ground. *GEOMATE Journal,* 11(26): 2633-2642.

[18] Aljanabi, K. R., & AL-Azzawi, O. M. 2021. Neural network application in forecasting maximum wall deflection in homogenous clay. International *Journal of Geo-Engineering*, 12, 1-18. DOI: https://doi.org/10.1186/s40703-021-00158-z

[19] Zhang, Z., Huang, M., & Wang, W. 2013. Evaluation of deformation response for adjacent tunnels due to soil unloading in excavation engineering. *Tunnelling and Underground Space Technology*, 38: 244-253. DOI: https://doi.org/10.1016/j.tust.2013.07.002.

[20] Yang, X., Jia, M., & Ye, J. 2020. Method for estimating wall deflection of narrow excavations in clay. *Computers and Geotechnics,* 117: 103224. DOI: https://doi.org/10.1016/j.compgeo.2019.103224.

[21] Khoiri, M., & Ou, C. Y. 2013. Evaluation of deformation parameter for deep excavation in sand through case histories. Computers and Geotechnics, 47: 57-67. DOI: https://doi.org/10.1016/j.compgeo.2012.06.009.

[22] Long, M. 2001. Database for retaining wall and ground movements due to deep excavations. Journal of Geotechnical and Geoenvironmental Engineering, 127(3): 203-224. DOI: https://doi.org/10.1061/(ASCE)1090-0241(2001)127:3(203.

[23] Xiao, H., Zhou, S., & Sun, Y. 2019. Wall deflection and ground surface settlement due to excavation width and foundation pit classification. *KSCE Journal of Civil Engineering*, 23: 1537-1547. DOI: https://doi.org/10.1007/s12205-019-1712-8.

[24] Mei, Y., Zhou, D., Wang, X., Zhao, L., Shen, J., Zhang, S., & Liu, Y. 2021. Deformation law of the diaphragm wall during deep foundation pit construction on lake and sea soft soil in the Yangtze River Delta. *Advances in Civil Engineering*, 2021(1): 6682921. DOI: https://doi.org/10.1155/2021/6682921.

[25] Ou, C. Y., & Hsieh, P. G. 2011. A simplified method for predicting ground settlement profiles induced by excavation in soft clay. Computers and Geotechnics, 38(8): 987-997. DOI: https://doi.org/10.1016/j.compgeo.2011.06.008.

[26] Hsiung, B. C. B., Yang, K. H., Aila, W., & Hung, C. 2016. Three-dimensional effects of a deep excavation on wall deflections in loose to medium dense sands. *Computers and Geotechnics,* 80: 138-151.DOI: https://doi.org/10.1016/j.compgeo.2016.07.001.

[27] Hsiung, B. C. B., Yang, K. H., Aila, W., & Ge, L. 2018. Evaluation of the wall deflections of a deep excavation in Central Jakarta using three-dimensional modeling. *Tunnelling and Underground Space Technology*, 72: 84-96. DOI: https://doi.org/10.1016/j.tust.2017.11.013.

[28] Hung, N. K., & Phienwej, N. 2016. Practice and experience in deep excavations in soft soil of Ho Chi Minh City, Vietnam. *KSCE Journal of Civil Engineering*, 20: 2221-2234. DOI: https://doi.org/10.1007/s12205-015-0470-5.

[29] Duc, T. N. 2022. Soft Clay Stiffness Measured in Ho Chi Minh City with Oedometer Tests for Deep Excavation Calculation. In CIGOS 2021, Emerging Technologies and Applications for Green Infrastructure: Proceedings of the 6th International Conference on Geotechnics, Civil Engineering and Structures. 1181-1189. Springer Singapore. DOI: https://doi.org/10.1007/978-981-16-7160-9_120.

[30] Nguyen, B. P., Ngo, C. P., Tran, T. D., Bui, X. C., & Doan, N. P. 2022. Finite element analysis of deformation behavior of deep excavation retained by diagram wall in Ho Chi Minh city. *Indian Geotechnical Journal*, 52(4): 989-999. DOI: https://doi.org/10.1007/s40098-022-00611-5.

[31] Lai, V. Q., Le, M. N., Huynh, Q. T., & Do, T. H. 2020. Performance analysis of a combination between D-wall and Secant pile wall in upgrading the depth of basement by Plaxis 2D: a case study in *Ho Chi Minh city. In ICSCEA 2019: Proceedings of the International Conference on Sustainable Civil Engineering and Architecture.* 745-755. Springer Singapore. DOI: https://doi.org/10.1007/978-981-15-5144-4_72.

[32] Liu, W., Shi, P., Cai, G., & Gan, P. 2022. A three-dimensional mechanism for global stability of slurry trench in frictional soils. *European Journal of Environmental and Civil Engineering,* 26(2): 594-619. DOI: https://doi.org/10.1080/19648189.2019.1667876.

[33] Liu, W., Shi, P., Cai, G., & Cao, C. 2021. Seepage on local stability of slurry trench in deep excavation of diaphragm wall construction. *Computers and Geotechnics,* 129 : 103878. DOI: https://doi.org/10.1016/j.compgeo.2020.103878

[34] Aye, Z. Z., Boonyarak, T., Thasnanipan, N., & Prongmanee, N. 2015. Diaphragm wall support deep-excavations for underground space in Bangkok subsoil. In *Proceedings of the International Conference & Exhibition on Tunnelling & Underground Space (ICETUS2015),* Kuala Lumpur, Malaysia. 3-5.

[35] Tran, D., Nguyen, H., Wang, Y., Phan, K., Phu, T., Le, D., & Nguyen, T. (2023). Analysis of artificial intelligence approaches to predict the wall deflection induced by deep excavation. *Open Geosciences,* 15(1): 20220503. DOI: https://doi.org/10.1515/geo-2022-0503.

[36] Nguyen, T., & Pipatpongsa, T. 2020. Plastic behaviors of asymmetric prismatic sand heaps on the verge of failure. *Mechanics of Materials*, 151 : 103624. DOI: https://doi.org/10.1016/j.mechmat.2020.103624.

[37] Taborda, D. M., Pedro, A. M., & Pirrone, A. I. 2022. A state parameter-dependent constitutive model for sands based on the Mohr-Coulomb failure criterion. *Computers and Geotechnics*, 148 : 104811. DOI: https://doi.org/10.1016/j.compgeo.2022.104811.

[38] Moradi, R., Marto, A., Rashid, A. S. A., Moradi, M. M., Ganiyu, A. A., & Horpibulsuk, S. 2018. Bearing capacity of soft soil model treated with end-bearing bottom ash columns. *Environmental earth sciences,* 77 : 1-9. DOI: https://doi.org/10.1007/s12665-018-7287-8.

[39] Grujicic, M., Snipes, J. S., Ramaswami, S., & Yavari, R. 2013. Discrete element modeling and analysis of structural collapse/survivability of a building subjected to improvised explosive device (IED) attack. *Advances in Materials Science and Applications*, 2(1) : 9-24.

[40] Vaziri, M. 2024. Soil–structure interaction. In *Structural Design of Buildings: Holistic Design*. 105-13. Emerald Publishing Limited.

[41] Rahman, N. R., Rokonuzzaman, M., & Rahman, S. A.2025. Case Study on the Lateral Soil Movement of Pile Supported Bridge Abutment Constructed on Soft Soil. Available at SSRN 4792091.

[42] Saleh, S., Mohd Yunus, N. Z., Ahmad, K., & Mat Said, K. N. 2021. Numerical simulation with hardening soil model parameters of marine clay obtained from conventional tests. *SN Applied Sciences*, 3 : 1-13. DOI: https://doi.org/10.1007/s42452-020-04115-w.

[43] Wani, K. M. N. S., & Showkat, R. 2018. Soil constitutive models and their application in geotechnical engineering: a review. *International Journal of Engineering Research & Technology* 7(04): 137-145. DOI: https://doi.org/10.17577/IJERTV7IS040129

[44] Kempfert, H. G., & Gebreselassie, B. 2006. Constitutive soil models and soil parameters. *Excavations and Foundations in Soft Soils*, 57-116. DOI: https://doi.org/10.1007/3-540-32895-5_3.

[45] Henann, D. L., & Anand, L. 2009. A large deformation theory for rate-dependent elastic–plastic materials with combined isotropic and kinematic hardening. *International Journal of Plasticity*, 25(10) : 1833-1878. DOI: https://doi.org/10.1016/j.ijplas.2008.11.008.

[46] Schanz, T., Vermeer, P. A., & Bonnier, P. G. (2019). The hardening soil model: Formulation and verification. In *Beyond 2000 In Computational Geotechnics*. 281-296. Routledge.

[47] Contreras, U., Li, G., Foster, C. D., Shabana, A. A., Jayakumar, P., & Letherwood, M. D. 2012. Soil models survey and vehicle system dynamics. In I*nternational Design Engineering Technical Conferences and Computers and Information in Engineering Conference*. 45059: 623-640. American Society of Mechanical Engineers. DOI: https://doi.org/10.1115/DETC2012-71450.

[48] Ramm, E., Erhart, T., & Wall, W. A. 2007. Numerical modeling of transient impact processes with large deformations and nonlinear material behavior. In *Computational Plasticity*, 123-144. Springer Netherlands. DOI: https://doi.org/10.1007/978-1-4020-6577-4_8.

[49] Ren, Q., & Zhou, J. 2021. Numerical Modeling of Soil Constitutive Relationship. Springer. DOI: https://doi.org/10.1007/978-981-16-3231-0.

[50] Yao, Y. P., Liu, L., Luo, T., Tian, Y., & Zhang, J. M. 2019. Unified hardening (UH) model for clays and sands. *Computers and Geotechnics,* 110 : 326-343. DOI: https://doi.org/10.1016/j.compgeo.2019.02.024.

Appendix

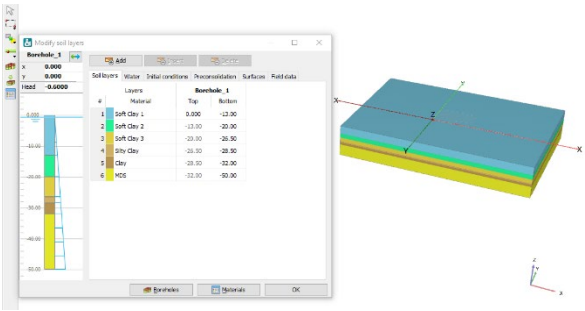

A1. Simulation of the ground model

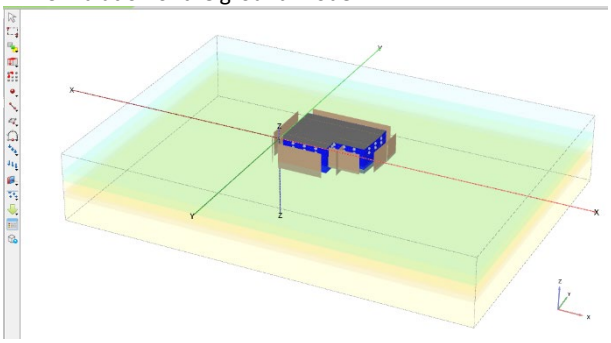

A2. Simulation of main structures for excavations

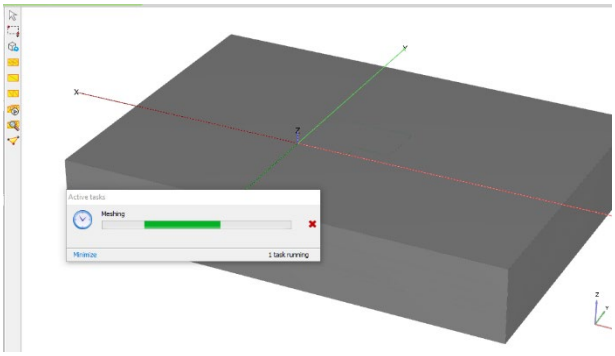

A3. Initial stress analysis for the model

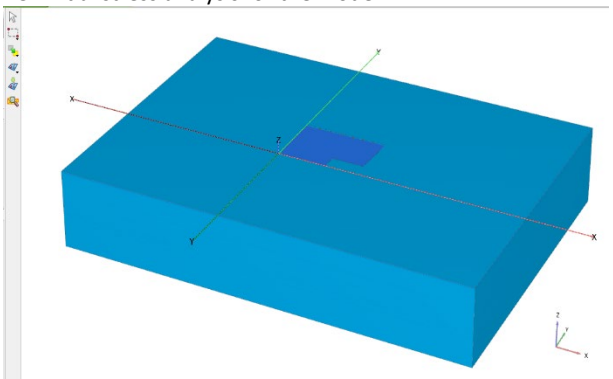

A4. Creating hydraulic conditions for the model

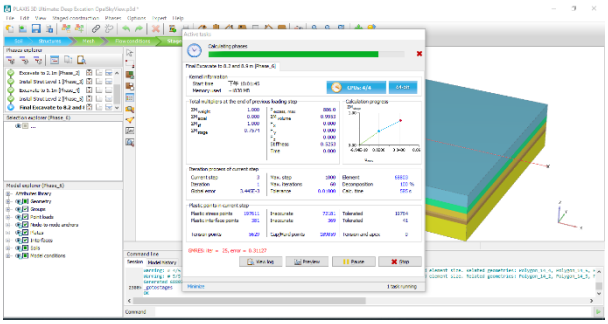

A5. Construction of excavation steps and analysis

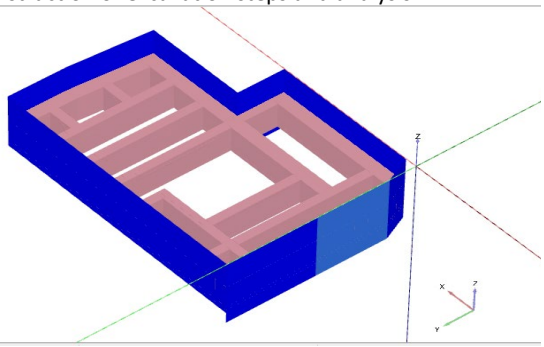

A6. Building CDM system

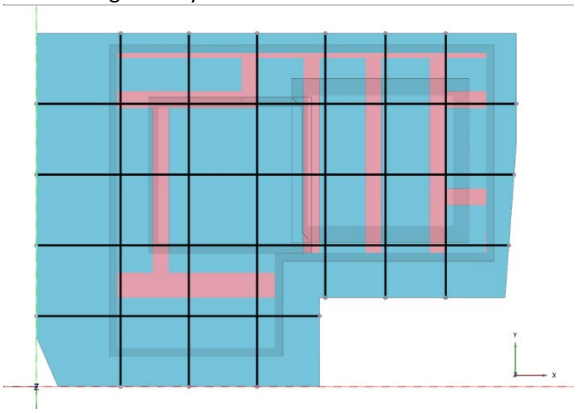

A7. Surface of the construction at the sixth phase excavation stage